



## Regular article

## Dislocation dipole-induced strengthening in intermetallic TiAl



Yan He<sup>a,b</sup>, Zhao Liu<sup>a</sup>, Gang Zhou<sup>a,c</sup>, Hao Wang<sup>a,\*</sup>, Chunguang Bai<sup>a</sup>, David Rodney<sup>d,1</sup>, Fritz Appel<sup>e</sup>, Dongsheng Xu<sup>a</sup>, Rui Yang<sup>a</sup>

<sup>a</sup> Institute of Metal Research, Chinese Academy of Sciences, 110016 Shenyang, China

<sup>b</sup> College of Physics and Technology, Shenyang Normal University, 110034 Shenyang, China

<sup>c</sup> School of Materials Science and Engineering, Dalian University of Technology, 116024 Dalian, China

<sup>d</sup> Institut Lumière Matière, Université Lyon 1, CNRS, UMR 5306, F-69622 Villeurbanne, France

<sup>e</sup> Institute for Materials Research, Helmholtz-Zentrum Geesthacht, D-21502 Geesthacht, Germany

## ARTICLE INFO

## Article history:

Received 18 May 2017

Received in revised form 27 July 2017

Accepted 6 September 2017

Available online xxxx

## Keywords:

Plasticity

Dislocation

Atomistic simulation

Intermetallics

Faulted dipole

## ABSTRACT

Narrow dislocation dipoles in intermetallic TiAl are systematically investigated by atomic-scale simulations and electron microscopy. The formation energy of narrow dipolar configurations and the activation energy during their evolution are unraveled. We show that faulted dipoles can be stable over experimental timescales, in full agreement with high-resolution observations. Such stable atomic-scale structures provide a strengthening effect significantly larger than the elastic prediction, which deeply influences plasticity in TiAl.

© 2017 Acta Materialia Inc. Published by Elsevier Ltd. All rights reserved.

Deformation of  $\gamma$ -TiAl alloys is mainly carried by the glide of ordinary dislocations with Burgers vector  $\frac{1}{2}\langle 110 \rangle$  and a limited amount of mechanical twinning. Superdislocations with Burgers vectors  $\langle 101 \rangle$  and  $\frac{1}{2}\langle 11\bar{2} \rangle$ , which also occur in  $\gamma$ -TiAl, exhibit an asymmetric non-planar core spreading and high glide resistance [1,2]. The ordinary dislocation has a compact core, which makes cross slip easy. Thus, the screw components of the ordinary dislocations contain a high density of jogs at which dislocation dipoles and debris are trailed and terminated [3–5]. There is good consensus that this jog dragging mechanism, together with lattice friction (Peierls mechanism), largely determines the mobility of the ordinary dislocations. It has been demonstrated [5] that the jog dragging significantly contributes to strain hardening at ambient temperatures. The stability of dipole structures is important for the evolution of internal stresses [6,7], dynamic recovery [8] and the temperature retention of strain hardening [5]. Dipole and debris structures were frequently observed in deformed TiAl alloys by transmission electron microscopy (TEM) [5,9–16]; however, the fine structure of the dipoles and their transformation into point defects are largely unknown. These aspects are addressed in the present study, where we have systematically examined the formation energy of narrow dipolar

configurations and the activation energy during their evolution employing empirical interatomic potentials, covering various dipole heights and orientations. The results are compared with TEM observations in the  $\gamma$  phase of different TiAl alloys. Lastly, the influence on plastic deformation is revealed with dislocation dipole-induced hardening beyond elastic prediction.

Dipole stability was first studied by classical molecular dynamics (MD). Vacancy- and interstitial-type dislocation dipoles in  $\gamma$ -TiAl, with Burgers vectors  $\pm \frac{1}{2}[1\bar{1}0]$ , heights  $1d$  to  $4d$  ( $d$  is the interplanar distance along  $[111]$ ) and orientation angles  $90^\circ$ ,  $74^\circ$ ,  $60^\circ$ ,  $41^\circ$  and  $30^\circ$  (defined as the angle between the Burgers vector and the dislocation line), were constructed using the methodology developed in Refs. [3,4]. Periodic boundary conditions were employed with simulation box dimensions  $6[\bar{1}\bar{1}2]$  by  $20[1\bar{1}0]$  by  $15[111]$ . Simulations were repeated in larger boxes to ensure negligible influence from the box size. An embedded-atom interatomic potential for the Ti–Al system [17] was employed. Fig. 1 shows the formation energy per vacancy/interstitial of various dipoles under low temperature relaxation. Vacancy dipoles are systematically more energetically stable than interstitial dipoles. Despite certain unexpected behavior of  $30^\circ$  vacancy and interstitial dipoles at  $2d$  and  $1d$ , respectively, all  $60^\circ$  vacancy dipoles, except at  $2d$ , possess the lowest formation energy at any given height. We therefore focus in the following on  $60^\circ$  vacancy dipoles. Their atomic configurations relaxed at 1 K for 50 ps and 1700 K for 1 ns are shown in Fig. 1c1–c4 and d1–d4, respectively. At 1 K, while the  $3d$  (Fig. 1c3) and  $4d$  (Fig. 1c4)

\* Corresponding author.

E-mail address: [haowang@imr.ac.cn](mailto:haowang@imr.ac.cn) (H. Wang).

<sup>1</sup> Prof. David Rodney was an editor of the journal during the review period of the article. To avoid a conflict of interest, Prof. I. Beyerlein acted as editor for this manuscript.

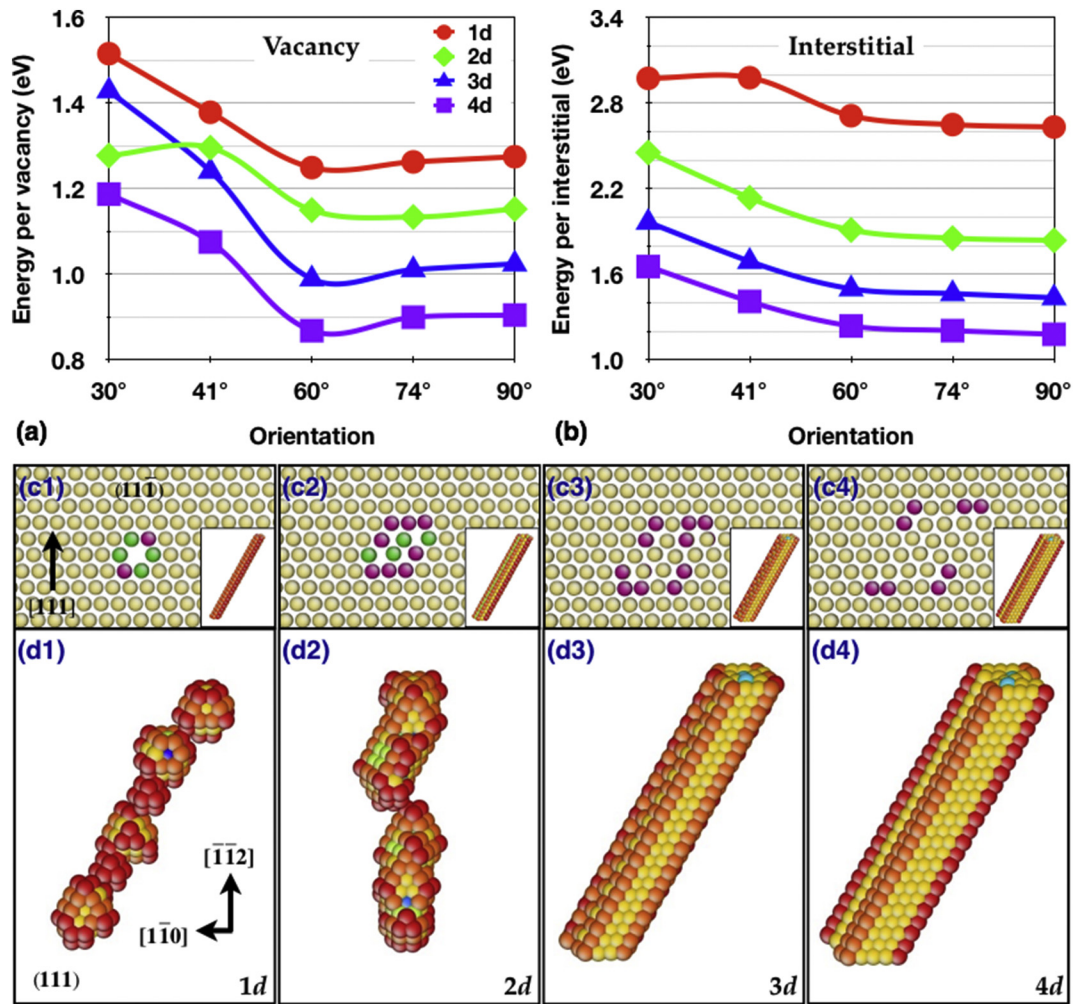


**Fig. 1.** (a/b) Formation energy per vacancy/interstitial of dipoles of various heights and orientations. Note the local minima at 60°. (c–d) Atomic configurations of 60° dipoles with heights 1d to 4d relaxed at 1 K for 50 ps (c1–c4) and at 1700 K for 1 ns (d1–d4). Atoms are colored according to their coordination number (c1–c4) or FCC-coordination number (d1–d4). Lattice orientations are indicated. (For interpretation of the references to color in this figure legend, the reader is referred to the web version of this article.)

dipoles stabilize as faulted dipoles [14], the 1d dipole becomes hollow and the 2d dipole is intermediate, with an open structure showing features of a faulted dipole. At 1700 K, the 3d and 4d 60°-dipoles remain stable and retain their low-temperature configurations within relaxation times up to 1 ns (Fig. 1d3 and d4), while significant atomic diffusion occurs in 1d and 2d dipoles (Fig. 1d1 and d2). Atoms are colored according to their coordination number (Fig. 1c1–c4) or FCC-coordination number (Fig. 1d1–d4) using AtomEye [18].

Such high stability of the 3d and 4d dipoles coincides with experimental observations of wide and narrow faulted dipoles under TEM (Fig. 2a, also see Fig. 5 in Ref. [14]) and high resolution TEM (Fig. 2b) [5], respectively. A characteristic feature is a dense structure of dislocation dipoles with a size distribution varying from 200 nm down to vanishingly small loops, which are referred to collectively as debris. The origin of a dipole is often traceable back to ordinary dislocations, which suggests that it was trailed and terminated at a jogged screw dislocation. The dipoles are almost perpendicularly elongated with respect to the Burgers vector, i.e., the two dipole arms have edge character and are situated on parallel glide planes. The detailed configuration depends on the height of the jog from which the dipole was trailed. At a sufficiently high stress, a screw dislocation may drag a mono-atomic jog along, which will leave behind a trail of vacancies or interstitial atoms depending on the sign of the dislocation and the direction the

dislocation is moving along. At taller jogs, dislocation dipoles are trailed as the screw dislocation moves, i.e., the jog is connected to the moving dislocation by two lengths of edge dislocations of opposite signs. Because of the mutual attraction of the positive and negative edge dislocations forming the dipole, a dipole may break up in a row of prismatic loops. Widely separated dipole arms may overcome their elastic interaction and operate as single-ended dislocation sources, for details see [5]. As an example, Fig. 2a shows the structure of dislocation dipoles in extruded Ti-45Al-8Nb-0.2C (at.%), TNB-V2, produced during low cycle fatigue at  $T = 550^{\circ}\text{C}$ . The micrograph shows numerous dipoles of different heights; high dipoles are about to open under combined glide and climb forces. Arrow (1) indicates an ordinary  $\frac{1}{2}\langle 110 \rangle$  screw dislocation trailing a 90° dipole, and arrow (2) designates dislocation dipoles that act as single ended dislocation sources. The orientation of the Burgers vector is noted as “b”. Fig. 2b shows a small dislocation dipole with its two edge dislocation arms produced during room temperature compression in deformed Ti-48Al-2Cr (at.%) under high resolution TEM along the  $\langle 10\bar{1} \rangle$  direction (Appel et al. [5]). The dipole has vacancy character because the (111) slip planes of the unlike edge dislocations are separated by a few atomic spacing, with the extra half planes lying outside the dipole. Here the MD result agrees well with the experimental observation. Fig. 2c shows the MD-predicted 3d 60° dipole as in Fig. 1c3, but reoriented according to the TEM image of Fig. 2b. For

Download English Version:

<https://daneshyari.com/en/article/5443274>

Download Persian Version:

<https://daneshyari.com/article/5443274>

[Daneshyari.com](https://daneshyari.com)